

Computational Modelling of Magneto-Hydrodynamic Casson Nanofluid Flow Over an Exponentially Slendering Surface with Radiation and Heat Source

Prathi Vijaya Kumar¹, Shaik Mohammed Ibrahim² and Giulio Lorenzini^{3*}

^{1,2} Department of Mathematics, GITAM University, Visakhapatnam, Andhra Pradesh -530045, India

^{3*} Department of Engineering and Architecture, University of Parma, Parco Area delle Scienze 181/A 43124 Parma, Italy

***Corresponding Author:** Giulio Lorenzini, Department of Engineering and Architecture, University of Parma, Parco Area delle Scienze 181/A 43124 Parma, Italy

ABSTRACT

In this paper, a boundary value problem which models two dimensional electrically conducting Casson nanofluid over an exponentially slendering sheet with variable thickness is analyzed. The impacts of thermal radiation, heat source, Brownian motion and thermophoretic diffusion are accounted in the flow region. Suitable similarity transformation is applied to bring the ordinary differential equations from the governing partial differential equations. These equations along with boundary conditions are solved using homotopy analysis method (HAM). Effects of magnetic parameter (M), Casson parameter (β), velocity power index parameter (m), Brownian motion parameter (Nb), thermophoresis parameter (Nt), radiation parameter (R), heat source parameter (Q), Prandtl number (Pr) and Schmidt number (Sc) on velocity, temperature, concentration, friction factor, local Nusselt number and local Sherwood number are given using graphs and tables for $\chi = 0.0$ (exponentially stretching sheet) and $\chi \neq 0.0$ (exponentially slendering sheet). It is noticed that the flow over exponentially stretching sheet has more effect on heat transfer rate when compared with the flow over exponentially slendering sheet.

Keywords: Casson nanofluid, thermal radiation, variable thickness, exponentially slendering sheet, HAM.

HIGHLIGHTS

- Two dimensional electrically conducting Casson nanofluid over an exponentially slendering sheet with variable thickness is examined.
- Analytical solutions are obtained using homotopy analysis method.
- It is scrutinized that exponentially stretching sheet shows more impact on heat transfer rate when compared with exponentially slendering sheet.
- Exponentially slendering sheet shows more impact on mass transfer rate when compared with exponentially stretching sheet.

NOMENCLATURE

x, y	directions along and normal to the surface	q_w	surface heat flux
u, v	velocity components in x, y directions	$\chi = A \sqrt{\frac{(m+1)U_0}{2\nu L}}$	wall thickness parameter
$B = B_0 e^{\frac{x}{2L}}$	magnetic field	Nu_x	local Nusselt number
T	temperature of the fluid	Sh_x	local Sherwood number
k	thermal conductivity	$Q = \frac{2LQ_0}{\rho C_p U_w}$	heat source parameter

Computational Modelling of Magneto-Hydrodynamic Casson Nanofluid Flow Over an Exponentially Slendering Surface with Radiation and Heat Source

C_p	specific heat at constant pressure	$Sc = \frac{\nu}{D_B}$	Schmidt number
D_B	Brownian diffusion coefficient	Re_x	local Reynolds number
C	nanoparticle volume fraction	<i>Greek symbols</i>	
D_T	Thermophoretic diffusion coefficient	ν	kinematic viscosity
T_∞	ambient temperature	ρ	fluid density
Q_0	heat source coefficient	σ	Electrical conductivity
C_∞	ambient nanoparticle volume fraction	τ	ratio between the effective heat capacity of the nanoparticle material and heat capacity of the fluid
U_0	reference velocity	ψ	stream function
$U_w = U_0 e^{\frac{x}{L}}$	stretching velocity	η, ξ	similarity variables
$T_w(x)$	temperature at the surface	θ	dimensionless temperature in $[\chi, \infty)$
$C_w(x)$	nanoparticle concentration at the surface	Θ	dimensionless temperature with respect to $[0, \infty)$
A	coefficient related to exponentially stretching sheet	ϕ	dimensionless nanoparticle volume fraction in $[\chi, \infty)$
f	dimensionless stream function in $[\chi, \infty)$	Φ	dimensionless nanoparticle volume fraction with respect to $[0, \infty)$
F'	dimensionless fluid velocity with respect to $[0, \infty)$	μ	dynamic viscosity
L	reference length	μ_∞	ambient dynamic viscosity
m	velocity power index parameter	τ_w	wall shear stress
$M = \frac{2\sigma B_0^2}{\rho U_0}$	Magnetic parameter	j_w	surface mass flux
$Pr = \frac{\rho C_p}{\nu}$	Prandtl number	σ^*	Stefan-Boltzman constant
$Nb = \frac{\tau D_B (C - C_\infty)}{\nu}$	Brownian motion parameter	k^*	mean absorption coefficient
$Nt = \frac{\tau D_T (T - T_\infty)}{\nu T_\infty}$	thermophoresis parameter	<i>Subscripts</i>	
q_r	radiative heat flux	w	condition at the surface
β	Casson parameter	∞	condition at the free stream
$R = \frac{4\sigma^* T_\infty^3}{k^* k}$	radiation parameter		

INTRODUCTION

There has been expeditious development in the study of laminar boundary layer flow and heat transfer over a stretching surface in the presence of magnetic field due to their voluminous applications in different fields like in aerodynamics, extrusion of plastic sheets, glass blowing, cooling procedure of metallic sheets, glass fiber production, etc. Sakiadis [1] initiated the study of stretching flow problem. Crane [2] induced the study of two dimensional boundary layer flow in which velocity varies linearly with a distance from a fixed point. The problems of Sakiadis and Crane were widened by many researchers under various situations. Cortell [3] analyzed the heat transfer behaviour over a nonlinear stretching sheet. Rajnish and Nageswara Rao [4] proffered an amendment in the linearization of T^4 to glean the realistic complexion of temperature distribution.

Nanofluids have extensive uses in various scientific fields and industries due to their stable nature and free from other problems like sedimentation, erosion, additional pressure drop, etc. These fluids find applications in power generators, micro manufacturing, automobiles, etc. Tiwari and Das [5] and Moaiga et al. [6] deduced that thermal conductivity can be increased by the introduction of nanoparticles in the fluids and hence the features of heat transfer. Sheremet [7] obtained the numerical solutions for the free convection flow of nanofluid under thermal stratification. Das et al. [8] discussed the boundary layer slip flow and heat transfer of nanofluid over a stretching sheet. Mabood et al. [9] reported the properties of nanofluid flow over a nonlinear stretching sheet. Shehzad et al. [10] have taken the convective mass condition and analyzed the MHD boundary layer flow on nanofluid. Ramana Reddy et al. [11] observed the higher heat transfer rate in Ag-water when compared with TiO_2 -water nanofluid. Extensive literature on nanofluid flows can be found in [12-19].

Variable thickness sheets are generally used in machine design, nuclear reactor technology, architecture, etc. The concept of variable thickness sheet was initiated by Lee [20]. Fang et al. [21] applied this to the boundary layer flow. Anjali Devi and Prakash [22] studied the hydromagnetic flow properties over a variable thickness stretching sheet. Srinivas Reddy et al. [23] illustrated the impact of radiation on

Williamson nanofluid. Prasad et al. [24] reported that the nanofluid flow over a variable thickness stretching sheet decelerates with suction and opposite results exist with injection.

Casson fluid [25] is a non-Newtonian fluid which exhibits yield stress. It is a worthwhile model for many fluids such as blood, chocolate, honey, etc. Casson fluid constitutive equation delineate a nonlinear relationship among stress and rate of strain and has been observed to be perfectly admissible to silicon suspensions, suspensions of bentonite in water, and lithographic varnishes used for printing inks. Raju et al. [26] reported the heat and mass transfer behavior of MHD Casson fluid over an exponential permeable stretching surface. Ibrahim et al. [27] analyzed the mixed convection flow of Casson nanofluid with chemical reaction and heat source. The magnetohydrodynamic (MHD) stagnation point flow of Casson nanofluid over a nonlinear stretching sheet in the presence of velocity slip and convective boundary condition is studied by Ibrahim et al. [28]. Malik et al. [29] obtained the similarity solutions for the flow Casson nanofluid over a vertical cylinder which is stretched exponentially. Pramanik [30] studied the thermal radiation effect on Casson fluid past an exponentially porous stretching surface. Afify [31] studied the viscous dissipation and chemical reaction effects on Casson nanofluid.

Here we analyze the MHD flow over an exponentially slendering sheet with thermal radiation and heat source. In the mathematical model Brownian motion (Nb) and thermophoretic diffusion (Nt) of nanoparticles are considered. The obtained model was solved by HAM. It has been proved that this technique is a worthwhile approach in dealing with various problems [32-35].

MATHEMATICAL FORMULATION

Consider a steady two dimensional forced convection MHD Casson nanofluid over an exponentially slendering stretching sheet with variable thickness. Thermal radiation and heat source are considered in the energy equation. We also considered the combined effect of Brownian motion and thermophoresis. The stretching velocity at the free stream is of the

form $U_w = U_0 e^{\frac{x}{L}}$. The Casson fluid flow is assumed to occupy the domain $Ae^{-\frac{x}{2L}} \leq y < \infty$ as shown in the Fig. 1. It is also assumed that a

Computational Modelling of Magneto-Hydrodynamic Casson Nanofluid Flow Over an Exponentially Slendering Surface with Radiation and Heat Source

magnetic field of strength $B = B_0 e^{\frac{x}{2L}}$ is applied perpendicular to the Casson nanofluid flow. T_w and C_w are taken as the wall temperature and nanoparticle concentration, T_∞ and C_∞ are the ambient values of temperature and nanoparticle concentration.

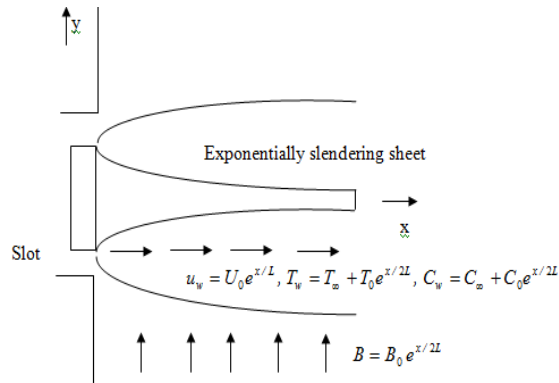


Figure 1. Coordinate system of the Casson nanofluid flow

Under the boundary layer approximations, the governing equations for of this problem can be expressed as

$$\frac{\partial u}{\partial x} + \frac{\partial v}{\partial y} = 0, \quad (1)$$

$$u \frac{\partial u}{\partial x} + v \frac{\partial u}{\partial y} = \nu \left(1 + \frac{1}{\beta} \right) \frac{\partial^2 u}{\partial y^2} - \frac{\sigma B(x)^2}{\rho} u, \quad (2)$$

$$u \frac{\partial T}{\partial x} + v \frac{\partial T}{\partial y} = \frac{k}{\rho C_p} \frac{\partial^2 T}{\partial y^2} - \frac{1}{\rho C_p} \frac{\partial q_r}{\partial y} + \tau \left[D_B \left(\frac{\partial C}{\partial y} \frac{\partial T}{\partial y} \right) + \frac{D_T}{T_\infty} \left(\frac{\partial T}{\partial y} \right)^2 \right] + \frac{Q_0}{\rho C_p} (T - T_\infty), \quad (3)$$

$$u \frac{\partial C}{\partial x} + v \frac{\partial C}{\partial y} = D_B \left(\frac{\partial^2 C}{\partial y^2} \right) + \frac{D_T}{T_\infty} \left(\frac{\partial^2 T}{\partial y^2} \right). \quad (4)$$

The boundary conditions are

$$u = U_w, \quad v = 0, \quad T = T_w, \quad C = C_w \quad \text{at} \quad y = A e^{-\frac{x}{2L}}, \quad (5)$$

$$u = 0, \quad T = T_\infty, \quad C = C_\infty, \quad \text{at} \quad y = \infty.$$

By using Rosseland approximation, we have

$$q_r = -\frac{4\sigma^*}{3k^*} \frac{\partial T^4}{\partial y}.$$

Taylor's series is utilized in taking the following expression

$$T^4 \cong 4T_\infty^3 T - 3T_\infty^4.$$

We assume that the surface is retained at a temperature and nanoparticle volume fraction

$$T_w = T_\infty + T_0 e^{\frac{x}{2L}} \theta(\eta), \quad C_w = C_\infty + C_0 e^{\frac{x}{2L}} \phi(\eta).$$

Now we induce the similarity transformations

$$\psi(x, y) = f(\eta) \sqrt{\frac{2\nu U_0 L}{m+1}} e^{\frac{x}{2L}}, \quad \eta = e^{\frac{x}{2L}} \sqrt{\frac{(m+1)U_0}{2\nu L}} y, \quad T = T_\infty + (T_w - T_\infty) \theta(\eta),$$

$$C = C_\infty + (C_w - C_\infty) \phi(\eta), \quad u = \frac{\partial \psi}{\partial x} = U_0 f'(\eta) e^{\frac{x}{2L}}, \quad (6)$$

$$v = -\frac{\partial \psi}{\partial y} = -\sqrt{\frac{\nu U_0}{2L(m+1)}} e^{\frac{x}{2L}} (f(\eta) + \eta f'(\eta))$$

Here u and v satisfy the continuity equation. Equations (2) to (5) become

The rheological equation of state for an isotropic and incompressible flow of a Casson fluid is

$$\tau_{ij} = \begin{cases} 2 \left(\mu_B + \frac{p_y}{\sqrt{2\pi}} \right) e_{ij}, & \pi > \pi_c \\ 2 \left(\mu_B + \frac{p_y}{\sqrt{2\pi_c}} \right) e_{ij}, & \pi_c > \pi \end{cases},$$

where μ_B is the dynamic viscosity of the non-Newtonian fluid, p_y is the yield stress of the fluid, π is the product of the component of deformation rate with itself, $\pi = e_{ij} e_{ij}$, e_{ij} is the $(i, j)^{th}$ component of the deformation rate and π_c is the critical value of this product based on the non-Newtonian model.

$$\left(1 + \frac{1}{\beta}\right) f'''' + \left(\frac{1}{m+1}\right) [f f'' - 2(f')^2 - M f'] = 0, \quad (7)$$

$$\left(1 + \frac{4R}{3}\right) \theta'' + Pr \left[\frac{1}{m+1} (f\theta' - f'\theta + Q\theta) + Nb\theta'\phi' + Nt\theta'^2 \right] = 0, \quad (8)$$

$$\phi'' + \frac{Nt}{Nb} \theta'' + \frac{Sc}{m+1} (f\phi' - f'\phi) = 0. \quad (9)$$

The boundary conditions are

$$\begin{aligned} f(\chi) = -\chi, \quad f'(\chi) = 1, \quad \theta(\chi) = 1, \quad \phi(\chi) = 1, \\ f'(\infty) = 0, \quad \theta(\infty) = 0, \quad \phi(\infty) = 0. \end{aligned} \quad (10)$$

To execute the calculations easily, we avail the functions $F(\xi) = F(\eta - \chi) = f(\eta)$, $\Theta(\xi) = \Theta(\eta - \chi) = \theta(\eta)$ and $\Phi(\xi) = \Phi(\eta - \chi) = \phi(\eta)$. Then the above equations take the form

$$\left(1 + \frac{1}{\beta}\right) F'''' + \left(\frac{1}{m+1}\right) [F F'' - 2(F')^2 - M F'] = 0, \quad (11)$$

$$\left(1 + \frac{4R}{3}\right) \Theta'' + Pr \left[\frac{1}{m+1} (F\Theta' - F'\Theta + Q\Theta) + Nb\Theta'\Phi' + Nt\Theta'^2 \right] = 0, \quad (12)$$

$$\Phi'' + \frac{Nt}{Nb} \Theta'' + \frac{Sc}{m+1} (F\Phi' - F'\Phi) = 0. \quad (13)$$

The boundary conditions are

$$\begin{aligned} F(0) = -\chi, \quad F'(0) = 1, \quad \Theta(0) = 1, \quad \Phi(0) = 1, \\ F'(\infty) = 0, \quad \Theta(\infty) = 0, \quad \Phi(\infty) = 0. \end{aligned} \quad (14)$$

In nanofluid problems, the physical quantities of interest are friction factor (C_f), wall heat transfer (Nu_x) and the volume fraction mass transfer (Sh_x) is defined as:

$$C_f = \frac{\tau_w}{\frac{1}{2} \rho U_w^2}, \quad Nu_x = \frac{x q_w}{k(T_w - T_\infty)}, \quad Sh_x = \frac{x j_w}{k(C_w - C_\infty)},$$

where $\tau_w = \mu \left(\frac{\partial u}{\partial y} \right)$, $q_w = -k \left(\frac{\partial T}{\partial y} \right)$, $j_w = -D_B \left(\frac{\partial C}{\partial y} \right)$ at $y = Ae^{-\frac{x}{2L}}$.

Using above quantities, we have

$$Re_x^{1/2} C_f = 2 \left(1 + \frac{1}{\beta}\right) \sqrt{\frac{m+1}{2}} F''(0), \quad Re_x^{-1/2} Nu_x = - \left(1 + \frac{4}{3} R\right) \left(\frac{x}{L}\right) \sqrt{\frac{m+1}{2}} \Theta'(0) \text{ and}$$

$$Re_x^{-1/2} Sh_x = - \left(\frac{x}{L}\right) \sqrt{\frac{m+1}{2}} \Phi'(0),$$

where $Re_x = \frac{U_w L}{\nu}$ is the local Reynolds number.

HAM

To build up the homotopic solutions of equations (11) to (14), we pick up the initial guesses and linear operators as follows

$$F_0(\xi) = -\chi + 1 + e^{-\xi},$$

$$\Theta_0(\xi) = e^{-\xi},$$

$$\Phi_0(\xi) = e^{-\xi},$$

$$L_1(F) = F'''' - F',$$

$$L_2(\Theta) = \Theta'' - \Theta,$$

$$L_3(\Phi) = \Phi'' - \Phi,$$

with

$$L_1(C_1 + C_2 e^\xi + C_3 e^{-\xi}) = 0,$$

$$L_2(C_4 e^\xi + C_5 e^{-\xi}) = 0,$$

$$L_3(C_6 e^\xi + C_7 e^{-\xi}) = 0,$$

where C_i ($i = 1$ to 7) are the arbitrary constants.

We construct the zeroth-order deformation equations

$$(1-p)L_1(F(\xi; p) - F_0(\xi)) = p\hbar_1 N_1[F(\xi; p)], \quad (15)$$

$$(1-p)L_2(\Theta(\xi; p) - \Theta_0(\xi)) = p\hbar_2 N_2[F(\xi; p), \Theta(\xi; p), \Phi(\xi; p)], \quad (16)$$

$$(1-p)L_3(\Phi(\xi; p) - \Phi_0(\xi)) = p\hbar_3 N_3[F(\xi; p), \Theta(\xi; p), \Phi(\xi; p)], \quad (17)$$

subject to the boundary conditions

$$F(0; p) = -\chi, \quad F'(0; p) = 1, \quad F'(\infty; p) = 0, \quad (18)$$

$$\Theta(0; p) = 1, \quad \Theta(\infty; p) = 0,$$

$$\Phi(0; p) = 1, \quad \Phi(\infty; p) = 0,$$

where

$$N_1[F(\xi; p)] = \left(1 + \frac{1}{\beta}\right) \frac{\partial^3 F(\xi; p)}{\partial \xi^3} + \frac{1}{m+1} \left[\begin{aligned} &F(\xi; p) \frac{\partial^2 F(\xi; p)}{\partial \xi^2} - 2 \left(\frac{\partial F(\xi; p)}{\partial \xi} \right)^2 \\ &- M \frac{\partial F(\xi; p)}{\partial \xi} \end{aligned} \right], \quad (19)$$

$$N_2[F(\xi; p), \Theta(\xi; p), \Phi(\xi; p)] = \left(1 + \frac{4}{3}R\right) \frac{\partial^2 \Theta(\xi; p)}{\partial \xi^2} \quad (20)$$

$$+ Pr \left(\frac{1}{m+1} \left(F(\xi; p) \frac{\partial \Theta(\xi; p)}{\partial \xi} - \frac{\partial F(\xi; p)}{\partial \xi} \Theta(\xi; p) + Q \Theta(\xi; p) \right) + (Nb \Theta' \Phi' + Nt \Theta'^2) \right),$$

$$N_3[F(\xi; p), \Theta(\xi; p), \Phi(\xi; p)] = \frac{\partial^2 \Phi(\xi; p)}{\partial \xi^2} + \frac{Nt}{Nb} \frac{\partial^2 \Theta(\xi; p)}{\partial \xi^2} + \frac{Sc}{m+1} \left[\begin{aligned} &F(\xi; p) \frac{\partial \Phi(\xi; p)}{\partial \xi} \\ &- \frac{\partial F(\xi; p)}{\partial \xi} \Phi(\xi; p) \end{aligned} \right], \quad (21)$$

where $p \in [0,1]$ is the embedding parameter, \hbar_1, \hbar_2 and \hbar_3 are non-zero auxiliary parameters and N_1, N_2 and N_3 are nonlinear operators.

The nth-order deformation equations are follows

$$L_1(F_n(\xi) - \chi_n F_{n-1}(\xi)) = \hbar_1 R_n^F(\xi), \quad (22)$$

$$L_2(\Theta_n(\xi) - \chi_n \Theta_{n-1}(\xi)) = \hbar_2 R_n^\Theta(\xi), \quad (23)$$

$$L_3(\Phi_n(\xi) - \chi_n \Phi_{n-1}(\xi)) = \hbar_3 R_n^\Phi(\xi), \quad (24)$$

with the following boundary conditions

$$F_n(0) = 0, \quad F_n'(0) = 0, \quad F_n'(\infty) = 0, \quad (25)$$

$$\Theta_n(0) = 0, \quad \Theta_n(\infty) = 0,$$

$$\Phi_n(0) = 0, \quad \Phi_n(\infty) = 0,$$

where

$$R_n^F(\xi) = \left(1 + \frac{1}{\beta}\right) F_{n-1}'''' + \frac{1}{m+1} \left[\sum_{i=0}^{n-1} F_{n-1-i} F_i'' - 2 \sum_{i=0}^{n-1} F_{n-1-i}' F_i' - M F_{n-1}' \right], \quad (26)$$

$$R_n^\Theta(\xi) = \left(1 + \frac{4}{3}\right) \Theta_{n-1}'' + Pr \left[\begin{aligned} &\frac{1}{m+1} \left(\sum_{i=0}^{n-1} F_{n-1-i} \Theta_i' - \sum_{i=0}^{n-1} F_{n-1-i}' \Theta_i + Q \Theta_{n-1} \right) \\ &+ Nb \sum_{i=0}^{n-1} \Theta_{n-1-i}' \Phi_i' + Nt \sum_{i=0}^{n-1} \Theta_{n-1-i}' \Theta_i' \end{aligned} \right], \quad (27)$$

$$R_n^\Phi(\xi) = \Phi_{n-1}'' + \frac{Nt}{Nb} \Theta_{n-1}'' + \frac{Sc}{m+1} \left(\sum_{i=0}^{n-1} F_{n-1-i} \Phi_i' - \sum_{i=0}^{n-1} F_{n-1-i}' \Phi_i \right), \quad (28)$$

$$\chi_n = \begin{cases} 0, & n \leq 1, \\ 1, & n > 1. \end{cases} \quad (29)$$

Convergence of HAM

The auxiliary parameters \hbar_1, \hbar_2 and \hbar_3 controls and adjust the convergence of the obtained series solutions. To acquire the apt values for these parameters \hbar - curves are portrayed in Fig. 2. From this figure, the

presumable interval of auxiliary parameter is $[-1.4, 0.0]$.

The solutions are convergent for whole region of ξ when $\hbar_1 = \hbar_2 = \hbar_3 = -0.65$. Table. 1 shows the convergence of the method.

Computational Modelling of Magneto-Hydrodynamic Casson Nanofluid Flow Over an Exponentially Slendering Surface with Radiation and Heat Source

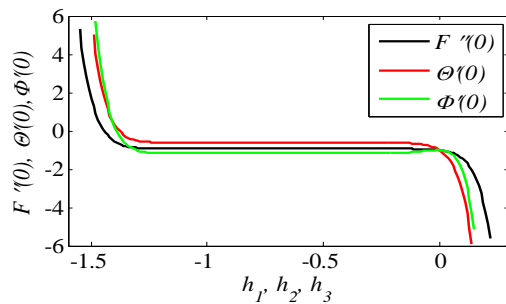


Figure 2. \bar{h} -curves of $F''(0)$, $\Theta'(0)$ and $\Phi'(0)$ for 15th order approximation.

Table 1. Convergence of HAM solutions for different orders of approximations when $\beta = 2.0, M = 0.5, m = 0.5, \chi = 0.2, R = 0.1, Pr = 2.0, Nb = 0.3, Nt = 0.2, Sc = 3.0, Q = 0.2$.

Order	$-f''(0)$	$-\Theta'(0)$	$-\Phi'(0)$
5	0.936668	0.613336	1.177725
10	0.936614	0.613506	1.175343
15	0.936612	0.613362	1.175846
20	0.936612	0.613443	1.175672
25	0.936612	0.613453	1.175740
30	0.936612	0.613463	1.175732
35	0.936612	0.613464	1.175727
40	0.936612	0.613464	1.175727
45	0.936612	0.613464	1.175727

RESULTS AND DISCUSSION

The percussion of retained pertinent parameters on the velocity, temperature, concentration, friction factor, local Nusselt number and local Sherwood number are explained.

For numerical solutions we considered the non-dimensional parameter values as

$$\beta = 2.0, M = 0.5, m = 0.5, \chi = 0.2, R = 0.1,$$

$$Pr = 2.0, Nb = 0.3, Nt = 0.2, Sc = 3.0, Q = 0.2.$$

These values are reserved in entire study apart from the variations in consequent figures and tables.

Raise in the magnetic parameter M proffers some boost to the resistance force known as Lorentz force which reduces the velocity and enhance the temperature and concentration in both $\chi = 0$ and $\chi \neq 0$. This is delineated in Figs. 3 to 5. Figs. 6 to 8 elucidate the proclivity of Casson parameter β on the distributions. It is seen that velocity decelerates and temperature and concentration raise with β . This appears duo to the increase of plastic dynamic viscosity with β . This is observed in both $\chi = 0$ and $\chi \neq 0$. Fig. 9 to 11 illustrate the impact of

velocity index parameter m on velocity, temperature and concentration. These distributions increase with m . This is due to the increase of slenderness in the sheet with m . This is observed in both $\chi = 0$ and $\chi \neq 0$.

Heat energy will be released with the increase of radiation parameter R as a result temperature increases with R . The thickness of the thermal boundary layer is much more in $\chi \neq 0$ than $\chi = 0$ case. This is represented in Fig. 12. Due to the slow rate of thermal diffusivity which is induced by the increasing values of Prandtl number Pr , temperature decreases and mixed behavior is observed for concentration profiles. It is observed that thickness of the thermal boundary layer is much bigger in $\chi \neq 0$ case compared to $\chi = 0$ case. This is elucidated in Figs. 13 and 14.

Fig. 15 presents the effects of the Brownian motion parameter Nb on the temperature profiles of the flow. It is observed that with the increment in Nb , temperature of the nanofluid increases in both $\chi = 0$ and $\chi \neq 0$ cases. This may happen since the Brownian motion enhances the colloidal fluid particle interaction. Physically when there is higher thickness in the sheet, particle to particle interaction is more. Hence flow over exponentially slendering sheet shows higher temperature profiles compared with exponentially stretching sheet. Fig. 16 depicts the influence of Nb on the concentration profiles of nanofluids. Increase in values of Nb shows reduction in nanoparticles diffusion for $\chi = 0$ and $\chi \neq 0$ cases. Figs. 17 and 18 demonstrate the effect of thermophoresis parameter Nt on temperature and concentration distributions. Rising values of Nt improve the temperature and concentration profiles for both $\chi = 0$ and $\chi \neq 0$ case. Physically due to movement of nanoparticles from hot to cold region with the increase of Nt causes increase in nanoparticle volume fraction and nanoparticle concentration boundary layer thickness.

Due to the production of heat energy in the flow region by the increment of heat source parameter Q temperature raises with Q . This is given in Fig. 19. Through Fig. 20, we illustrate the prepotency of Schmidt number Sc on concentration profiles. It is perceptible that an enhancement in Sc depreciates the concentration. This due to the lower molecular

diffusivity for the higher values of Sc . Impact of M and β on friction factor is shown in Fig. 21. It is seen that C_f decelerates by elevating the values of M and β . Fig. 22 explores the fluctuations of local Nusselt number for various values of Nb and Nt which decreases with the increase of Nb and Nt . From Fig. 23, it is noticed that local Nusselt number decreases with the increase of Q and R . Fig. 24 shows that local Sherwood number decreases by the increase of Pr and Sc .

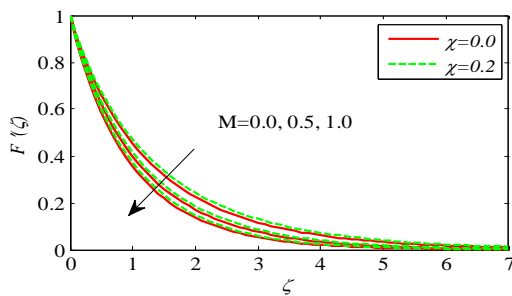


Figure3. Effect of M on $F'(\xi)$.

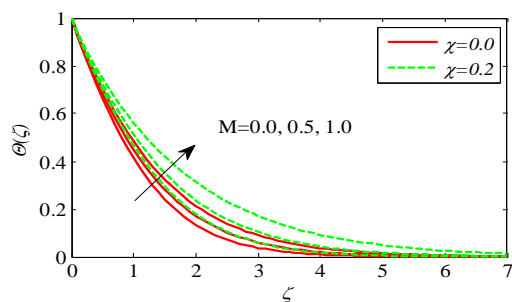


Figure4. Effect of M on $\Theta(\xi)$.

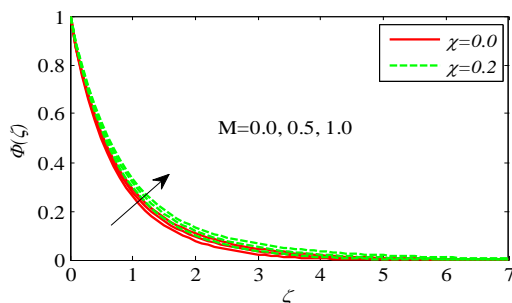


Figure5. Effect of M on $\Phi(\xi)$.

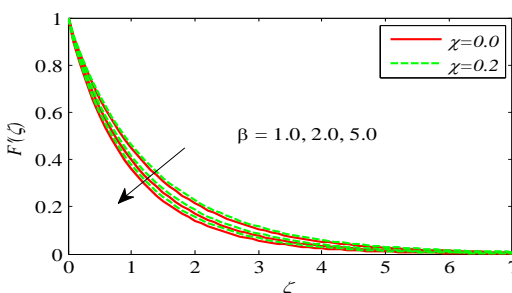


Figure6. Effect of β on $F'(\xi)$.

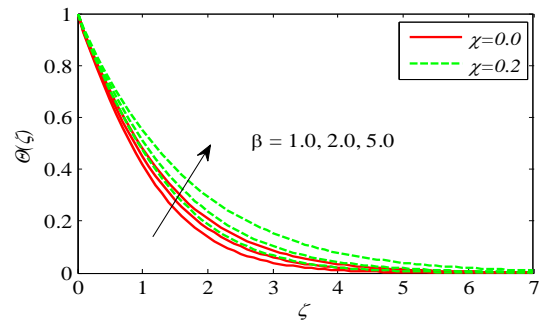


Figure7. Effect of β on $\Theta(\xi)$.

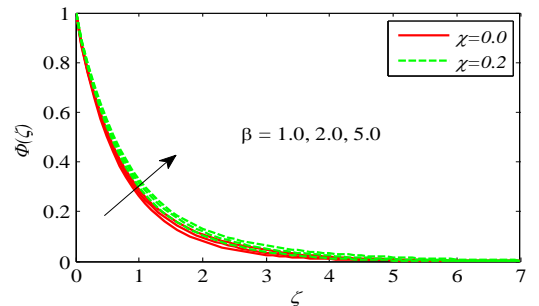


Figure8. Effect of β on $\Phi(\xi)$.

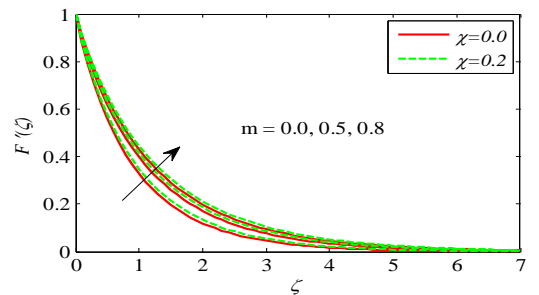


Figure9. Effect of m on $F'(\xi)$.

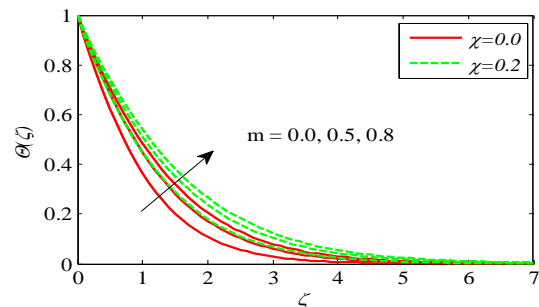


Figure10. Effect of m on $\Theta(\xi)$.

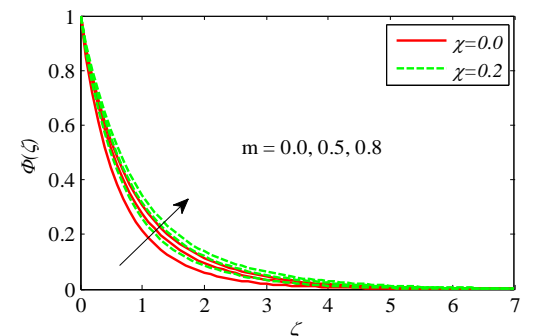


Figure11. Effect of m on $\Phi(\xi)$.

Computational Modelling of Magneto-Hydrodynamic Casson Nanofluid Flow Over an Exponentially Slendering Surface with Radiation and Heat Source

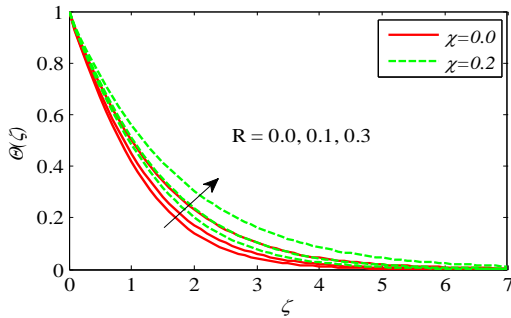


Figure12. Effect of R on $\Theta(\xi)$.

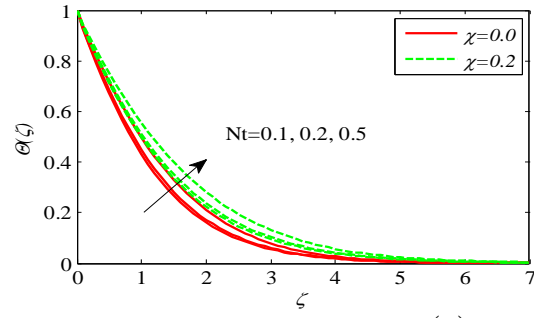


Figure17. Effect of Nt on $\Theta(\xi)$.

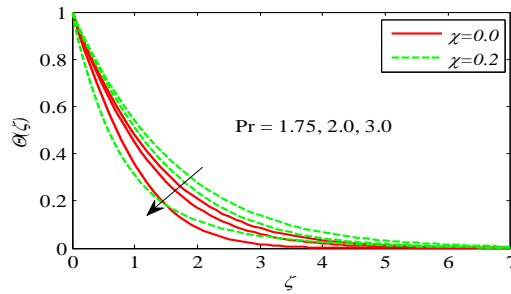


Figure13. Effect of Pr on $\Theta(\xi)$.

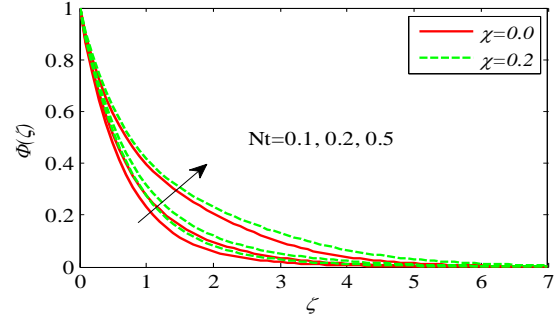


Figure18. Effect of Nt on $\Phi(\xi)$.

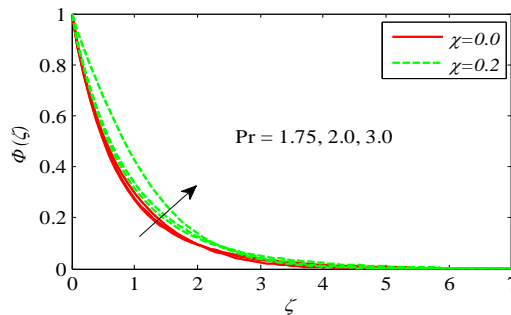


Figure14. Effect of Pr on $\Phi(\xi)$.

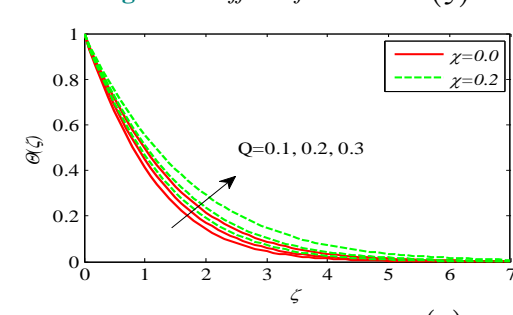


Figure19. Effect of Q on $\Theta(\xi)$.

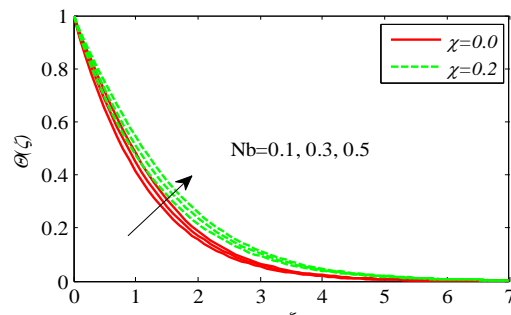


Figure15. Effect of Nb on $\Theta(\xi)$.

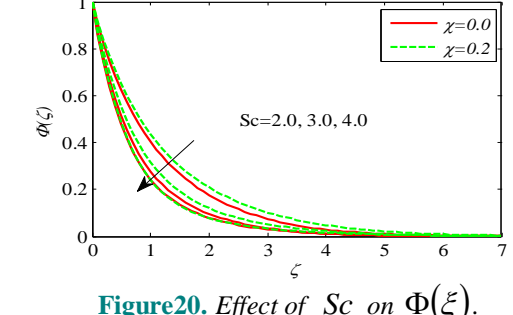


Figure20. Effect of Sc on $\Phi(\xi)$.

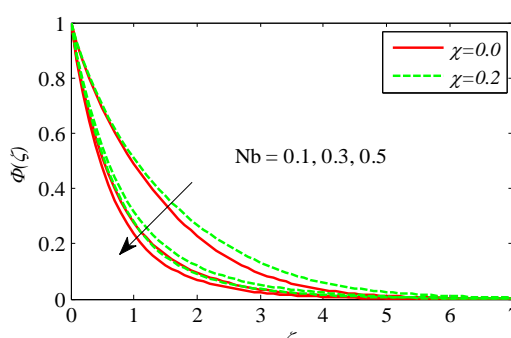


Figure16. Effect of Nb on $\Phi(\xi)$.

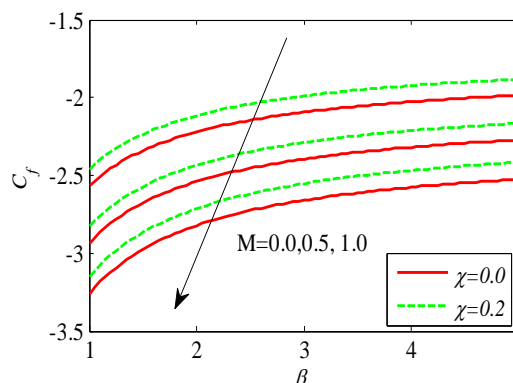


Figure21. Effect of M and β on C_f .

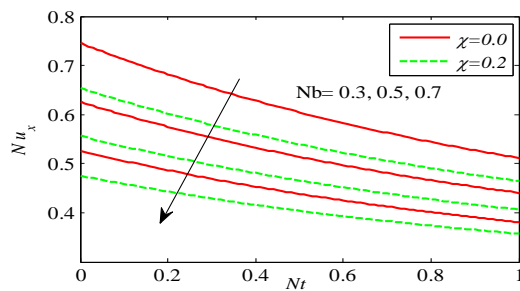


Figure 22. Effect of Nt and Nb on Nu_x .

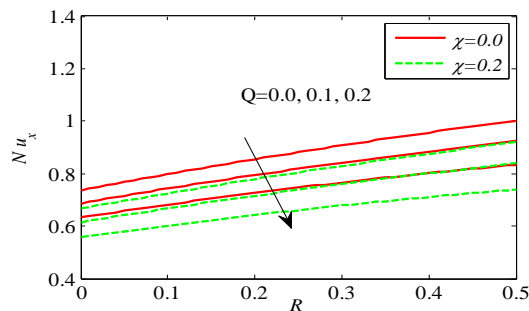


Figure 23. Effect of Q and R on Nu_x .

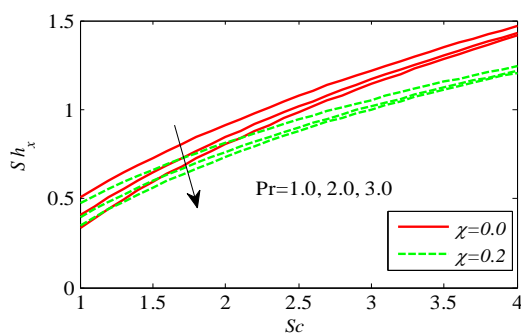


Figure 24. Effect of Pr and Sc on Sh_x .

In order to verify the accuracy and reliability of the present analysis, the obtained results have been compared with that of Bidin and Nazar [36] and Nadeem et al. [37] solutions for the limiting case when

$$M = 0.0, \beta \rightarrow \infty, m = 0.0, \chi = 0.0, Q = 0.0, Nb \rightarrow 0.0, Nt = 0.0$$

As shown in Table 2, the comparison in the above case is found to be in good agreement.

Table 2. Comparison of $-\Theta'(0)$.

Pr	R	Bidin and Nazar [36]	Nadeem et al. [37]	HAM
1.0	0.0	0.9547	--	0.954784
	0.5	0.6765	0.680	0.676511
	1.0	0.5315	0.534	0.531442
2.0	0.0	1.4714	--	1.471462
	0.5	1.0735	1.073	1.073520
	1.0	0.8627	0.863	0.862771

CONCLUSIONS

Here, we analyzed the MHD flow over an exponentially slandering sheet with radiation and heat source. In this procession, we delineated some graphs to perlustrate the pursuance of a few governing parameters on the flow field. The following conclusions have been made through this study.

- Nb and Nt are capable to magnify the temperature of the fluid.
- Enhancement in the velocity power index parameter index parameter exhibits the acceleration in velocity, temperature and concentration profiles.
- Immense thermal boundary layer is noticed in $\chi \neq 0$ when compared with $\chi = 0$.
- Schmidt number has propensity to decelerate the concentration field.
- There is a perceptible decrease in heat transfer rate with enhancing values of Q and R .

REFERENCES

- [1] B. S. Sakiadis, Boundary-layer behaviour on continuous solid surfaces, *American Institute of Chemical Engineers*, 7, 26-28, 1961.
- [2] L. J. Crane, Flow past a stretching sheet, *Zeitschrift für angewandte Mathematikund Physik*, 21, 645-647, 1970.
- [3] R. Cortell, Fluid flow and radiative nonlinear heat transfer over a stretching sheet, *Journal of King Saud University Science*, 26, 161-167, 2014.
- [4] Chava Y P D Phani Rajanish and B. Nageswara Rao, On the radiative heat transfer in a viscoelastic boundary layer flow over a stretching sheet, *Journal of Heat Transfer*, 139, 014501, 2016.
- [5] R. J. Tiwari and M. K. Das, Heat transfer augmentation in two-sided lid-driven differentially heated square cavity utilizing nanofluids, *International Journal of Heat and Mass Transfer*, 50, 2002-2018, 2007.
- [6] S. E. B. Maiga, S. J. Palm, C. T. Nguyen, G. Roy and N. Galanis, Heat transfer enhancement by using nanofluids in forced convection flows, *International Journal of Heat and Fluid Flow*, 26, 530-546, 2005.
- [7] M. A. Sheremet, S. Dinarvand and I. Pop, Effect of thermal stratification on free convection in a square porous cavity filled with nanofluid using Tiwari and Das'nanofluid model, *Physica E*, 69, 332-341, 2015.

- [8] S. Das, R. N. Jana and O. D. Makinde, MHD boundary layer slip flow and heat transfer of nanofluid past a vertical stretching sheet with non-uniform heat generation/absorption, *International Journal of Nanoscience*, 13, 1450019, 2014.
- [9] F. Mabood, W. A. Khan and A. I. M. Ismail, MHD boundary layer flow and heat transfer of nanofluids over a nonlinear stretching sheet: A numerical study, *Journal of Magnetism and Magnetic Materials*, 374, 569-576, 2015.
- [10] S. A. Shehzad, T. Hayat and A. Alsaedi, Influence of convective heat and mass conditions in MHD flow of nanofluid, *Bulletin of the Polish Academy of Sciences Technical Sciences*, 63, 465-474, 2015.
- [11] J. V. Ramana Reddy, V. Sugunamma, N. Sandeep and C. Sulochana, Influence of chemical reaction, radiation and rotation on MHD nanofluid flow past a permeable flat plate in porous medium, *Journal of the Nigerian Mathematical Society*, 35, 48-65, 2016.
- [12] S. Mansur and A. Ishak, Unsteady boundary layer flow of a nanofluid over a stretching/shrinking sheet with a convective boundary condition, *Journal of the Egyptian Mathematical Society*, 24, 650-655, 2016.
- [13] M. M. Bhatti and M. M. Rashidi, Effects of thermo-diffusion and thermal radiation on Williamson nanofluid over a porous shrinking/stretching sheet, *Journal of Molecular Liquids*, 221, 567-573, 2016.
- [14] Kai-Long Hsiao, Stagnation electrical MHD nanofluid mixed convection with slip boundary on a stretching surface, *Applied Thermal Engineering*, 98, 850-861, 2016.
- [15] M. Sheikholeslami, M. T. Mustafa and D. D. Ganji, Effect of Lorentz forces on forced-convection nanofluid over a stretched surface, *Particuology*, 26, 108-113, 2016.
- [16] S. P. Anjali Devi and P. Suriyakumar, Hydromagnetic mixed convective nanofluid slip flow past an inclined stretching plate in the presence of internal heat absorption and suction, *Journal of Applied Fluid Mechanics*, 9, 1409-1419, 2016.
- [17] Mohamed R. Eid, Chemical reaction effect on MHD boundary-layer flow of two-phase nanofluid model over an exponentially stretching sheet with heat generation, *Journal of Molecular Liquids*, 220, 718-725, 2016.
- [18] Y. M. Hung, Analytical study on forced convection of nanofluids with viscous dissipation in microchannels, *Heat Transfer Engineering*, 31, 1184-1192, 2010.
- [19] N. Sandeep and C. Sulochana, Dual solutions of radiative MHD nanofluid flow over an exponentially stretching sheet with heat generation/absorption, *Applied Nanoscience*, 6, 131-139, 2016.
- [20] L. Lee, Boundary layer flow over a thin layer, *Physics of Fluids*, 10, 820-822, 1967.
- [21] T. Fang, J. Zhang and Y. Zhong, Boundary layer flow over a stretching sheet with variable thickness, *Applied Mathematics and Computation*, 218, 7242-7252, 2012.
- [22] S. P. Anjali Devi and M. Prakash, Thermal radiation effects on hydromagnetic flow over a slendering stretching sheet, *Journal of Brazilian Society of Mechanical Sciences and Engineering*, 38, 423-431, 2016.
- [23] C. Srinivas Reddy, Kishan Naikoti and M. M. Rashid, MHD flow and heat transfer characteristics of Williamson nanofluid over a stretching sheet with variable thickness and variable thermal conductivity, *Transactions of A. Razmadze Mathematical Institute*, 171, 195-211, 2017.
- [24] K. V. Prasad, K. Vajravelu, Hanumesh Vaidya and Robert A. Van Gorder, MHD flow and heat transfer in a nanofluid over a slender elastic sheet with variable thickness, *Results in Physics*, 7, 1462-1474, 2017.
- [25] N. Casson, A flow equation for pigment oil suspensions of the printing ink type. In: Mill CC, *Rheology of Disperse Systems*, Pergamon press, New York, 84-104, 1959.
- [26] C. S. K. Raju, N. Sandeep, V. Sugunamma, M. Jayachandra Babu and J. V. Ramana Reddy, Heat and mass transfer in magnetohydrodynamic Casson fluid over an exponentially permeable stretching surface, *Engineering Science and Technology, an International Journal*, 19, 45-52, 2016.
- [27] S. M. Ibrahim, G. Lorenzini, P. Vijaya Kumar and C. S. K. Raju, Influence of chemical reaction and heat source on dissipative MHD mixed convection flow of a Casson nanofluid over a nonlinear permeable stretching sheet, *International Journal of Heat and Mass Transfer*, 111, 346-355, 2017.
- [28] S. M. Ibrahim, P. V. Kumar, G. Lorenzini, E. Lorenzini and F. Mabood, Numerical study of the onset of chemical reaction and heat source on dissipative mhd stagnation point flow of Casson nanofluid over a nonlinear stretching sheet with velocity slip and convective boundary conditions, *Journal of Engineering Thermophysics*, 26, 256-271, 2017.
- [29] M. Y. Malik, M. Naseer, S. Nadeem and Abdul Rehman, The boundary layer flow of Casson nanofluid over a vertical exponentially stretching cylinder, *Applied Nanoscience*, 4, 869-873, 2014.

Computational Modelling of Magneto-Hydrodynamic Casson Nanofluid Flow Over an Exponentially Slendering Surface with Radiation and Heat Source

- [30] S. Pramanik, Casson fluid flow and heat transfer past an exponentially porous stretching surface in presence of thermal radiation, *Ain Shams Engineering Journal*, 5, 205-212, 2014.
- [31] Ahmed A. Afify, The influence of slip boundary condition on Casson nanofluid flow over a stretching sheet in the presence of viscous dissipation and chemical reaction, *Mathematical Problems in Engineering*, 2017, 3804751, 2017.
- [32] S. J. Liao, Homotopy analysis method in nonlinear differential equations, *Springer & Higher Education Press*, Heidelberg, 2012.
- [33] T. Hayat, S. A. Shehzad and A. Alsaedi, Soret and Dufour effects on Magneto-hydrodynamic (MHD) flow of Casson fluid, *Applied Mathematics and Mechanics*, 33, 1301-1312, 2012.
- [34] Q. X. Liu, J. K. Liu and Y. M. Chen, Asymptotic limit cycle of fractional van der Pol oscillator by homotopy analysis method and memory-free principle, *Applied Mathematical Modelling*, 40, 3211-3220, 2016.
- [35] X. Zhong and S. Liao, On the homotopy analysis method for backward/forward-backward stochastic differential equations, *Numerical Algorithms*, 76, 487-519, 2017.
- [36] B. Bidin and R. Nazar, Numerical solution of the boundary layer flow over an exponentially stretching sheet with thermal radiation, *European Journal of Scientific Research*, 33, 710-717, 2009.
- [37] S. Nadeem, S. Zaheer and T. Fang, Effects of thermal radiation on the boundary layer flow of a Jeffrey fluid over an exponentially stretching surface, *Numerical Algorithms*, 57, 187-205, 2011.

Citation: P. Vijaya Kumar, S. Mohammed Ibrahim and G. Lorenzini, "Computational Modelling of Magneto-Hydrodynamic Casson Nanofluid Flow Over an Exponentially Slendering Surface with Radiation and Heat Source", vol. 5, no. 9, pp. 1-12, 2017.

Copyright: © 2017 G. Lorenzini, et al. This is an open-access article distributed under the terms of the Creative Commons Attribution License, which permits unrestricted use, distribution, and reproduction in any medium, provided the original author and source are credited.